SUPPORTING INFORMATION

Exploiting Protein Conformational Change to Optimize Adenosine-Derived Inhibitors of HSP70

Matthew D. Cheeseman,[1] Isaac M. Westwood,[1,2] Olivier Barbeau,[1] Martin Rowlands,[1] Sarah Dobson,[1,2] Alan M. Jones,[1] Fiona Jeganathan,[1] Rosemary Burke,[1] Nadia Kadi,[1] Paul Workman,[1] Ian Collins,[1] Rob L. M. van Montfort,[1,2] Keith Jones[1],*

[1] *Cancer Research UK Cancer Therapeutics Unit at The Institute of Cancer Research, London SW7 3RP, U.K.*

[2] *Division of Structural Biology at The Institute of Cancer Research, London SW7 3RP, U.K.*

Table of Contents

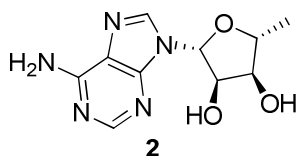**Commercially available adenosine analogues**
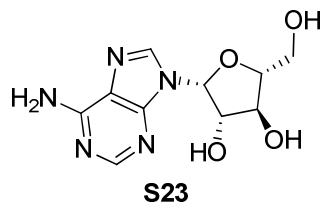The following compounds were purchased from commercial suppliers and used without further purification.

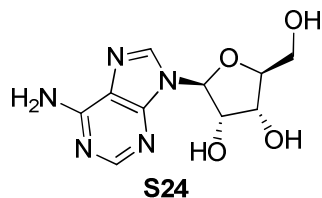

1
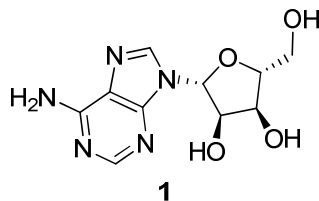
Adenosine 1 was purchased from Sigma-Aldrich

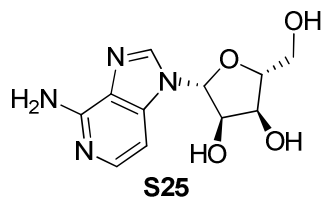**S22**
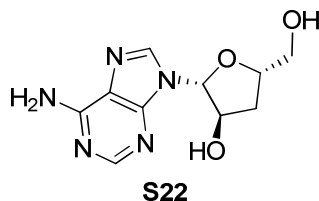
Cordycepin S22 was purchased from Sigma-Aldrich

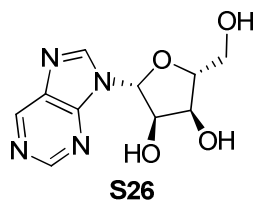
2

5'-Deoxyadenosine 2 was purchased from Carbosynth Limited
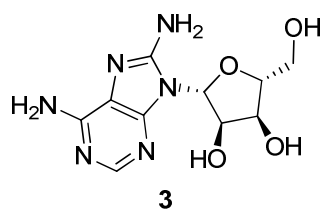
S23

*Vidarabine **S23** was purchased from Sigma-Aldrich*

S24

*L-Adenosine **S24** was purchased from Carbosynth Limited*
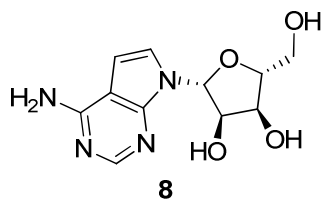

S25

*3-Deazaadenosine **S26** was purchased from Carbosynth Limited*
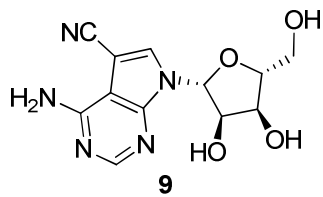

S26

*Nebularine **S27** was purchased from Carbosynth Limited*

3
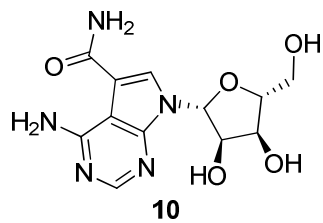
*8-Aminoadenosine **3** was purchased from Carbosynth Limited*
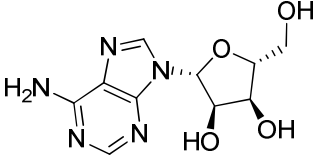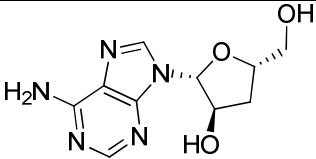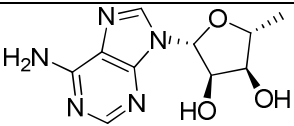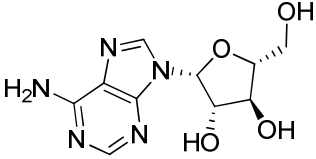

8

*Tubercidin **8** was purchased from Sigma-Aldrich*

9
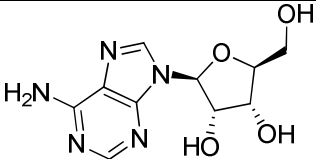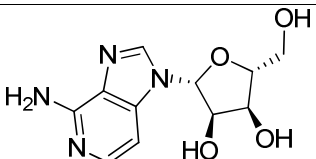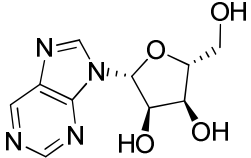
Toyocamycin 9 was purchased from Sigma-Aldrich

10

Sangivamycin 10 was purchased from Sigma-Aldrich

Supporting Information Table S1

Entry	Compd.	Structure	$pK_D \pm SEM^a$	$K_D (\mu M)^b$
1	**1**		3.95±0.01	110
2	**S23**		<3.00	>1000
3	**2**		3.88±0.02	130
4	**S24**		<3.00	>1000
5	**S25**		<3.00	>1000
6	**S26**		<3.00	>1000
7	**S27**		<3.00	>1000

[a]All results are quoted as the geometric mean±SEM of 3 independent experiments unless otherwise stated, $pK_D = -\log_{10}(K_D(\mu M) \ast 10^{-6})$. [b]All values are quoted to 2 significant figures.

NMR Spectra of final compounds

4
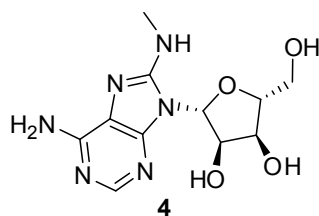
(2R,3R,4S,5R)-2-(6-amino-8-(methylamino)-9H-purin-9-yl)-5-(hydroxymethyl)tetrahydrofuran-3,4-diol 4

5
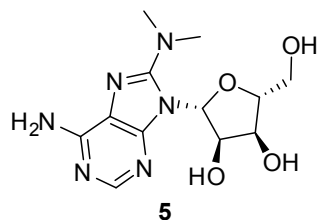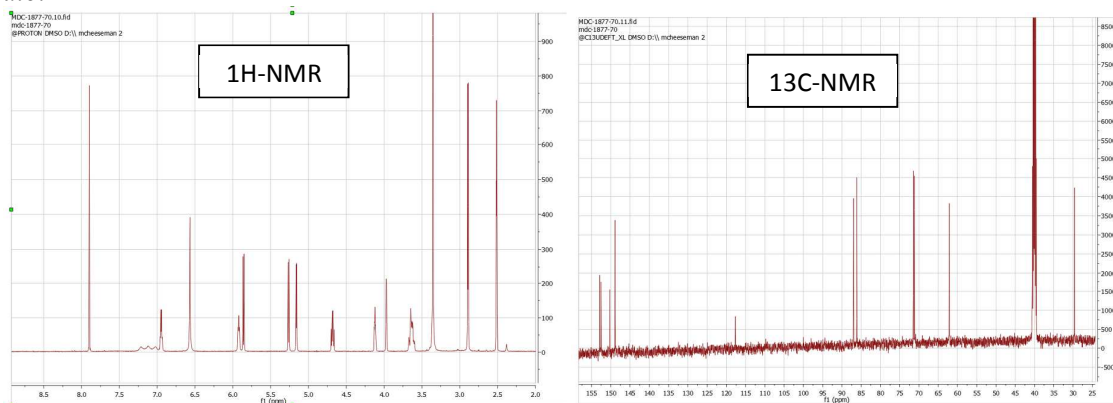
(2R,3R,4S,5R)-2-(6-amino-8-(dimethylamino)-9H-purin-9-yl)-5-(hydroxymethyl)tetrahydrofuran-3,4-diol 5

6
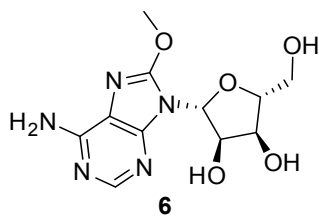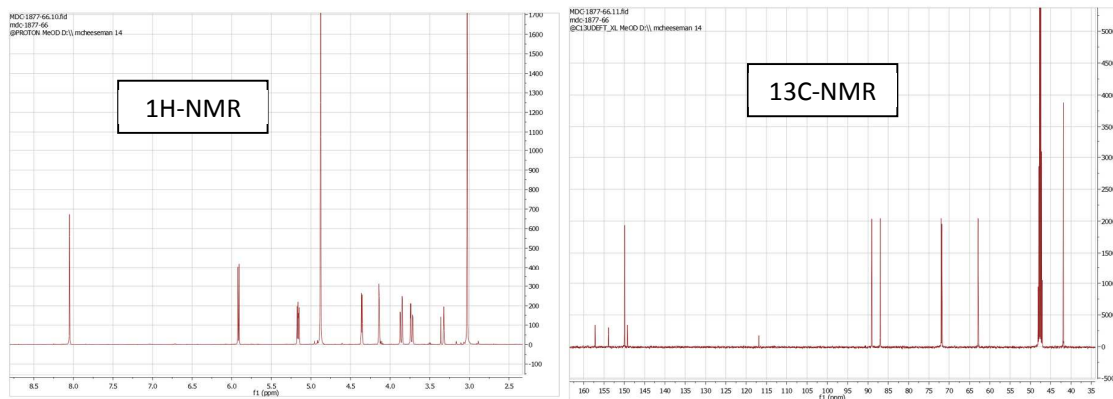
(2R,3R,4S,5R)-2-(6-amino-8-methoxy-9H-purin-9-yl)-5-(hydroxymethyl)tetrahydrofuran-3,4-diol 6

1H-NMR   13C-NMR
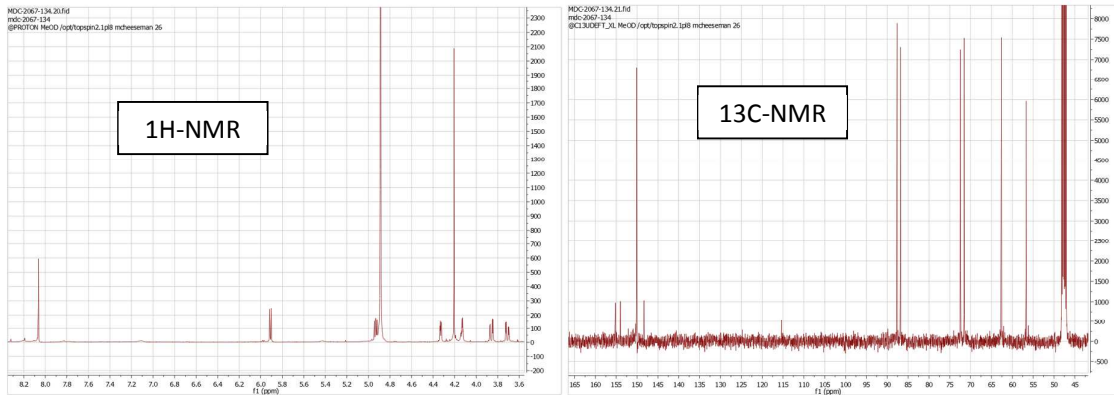
(2R,3R,4S,5R)-2-(6-amino-8-(methylamino)-9H-purin-9-yl)-5-methyltetrahydrofuran-3,4-diol **7**
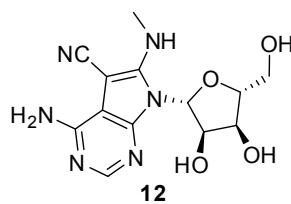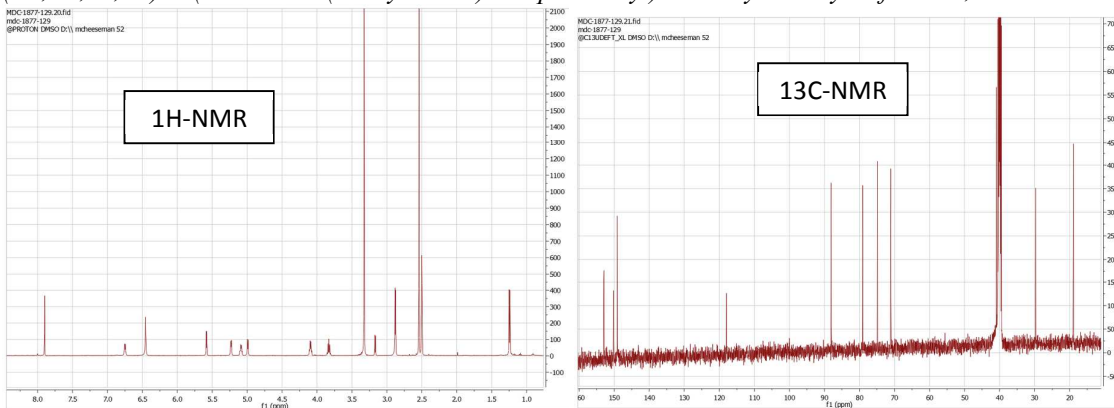
1H-NMR   13C-NMR

4-amino-7-((2R,3R,4S,5R)-3,4-dihydroxy-5-(hydroxymethyl)tetrahydrofuran-2-yl)-6-(methylamino)-7H-pyrrolo[2,3-d]pyrimidine-5-carbonitrile **12**
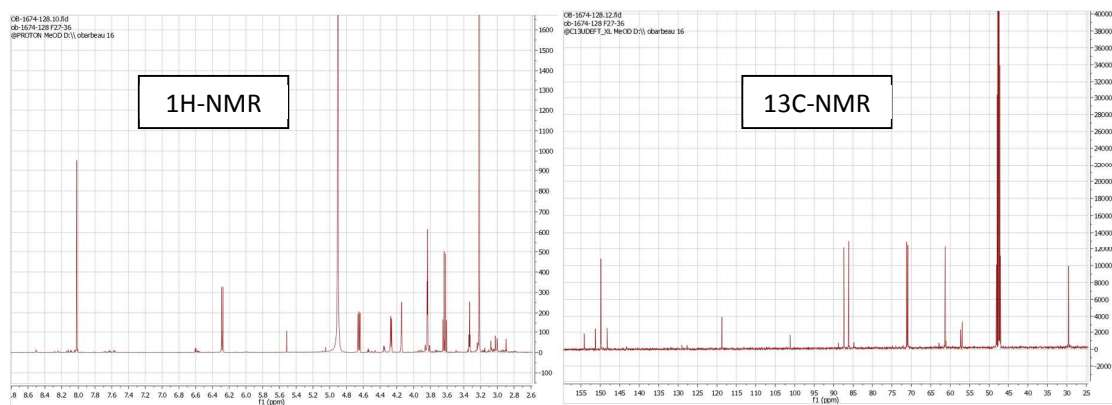
4-amino-7-((2R,3R,4S,5R)-3,4-dihydroxy-5-(hydroxymethyl)tetrahydrofuran-2-yl)-6-(methylamino)-7H-pyrrolo[2,3-d]pyrimidine-5-carboxamide 13
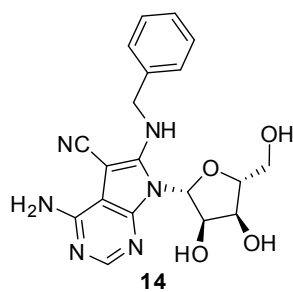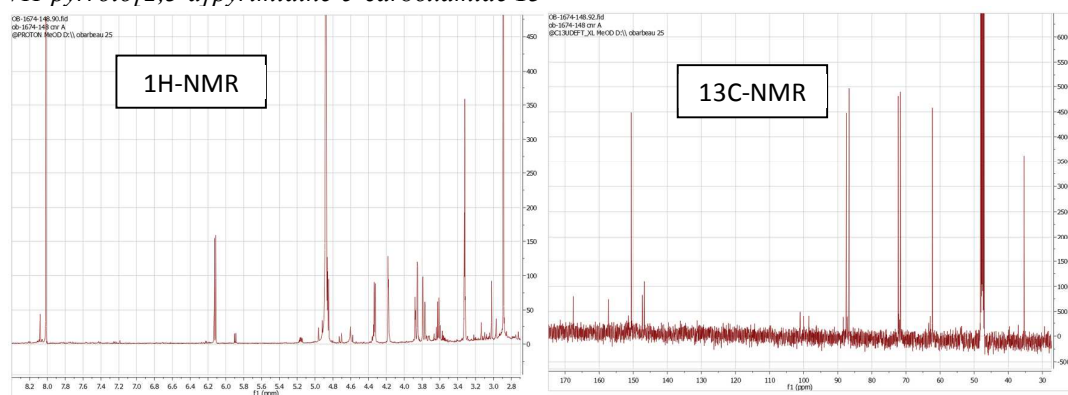
4-amino-6-(benzylamino)-7-((2R,3R,4S,5R)-3,4-dihydroxy-5-(hydroxymethyl)tetrahydrofuran-2-yl)-7H-pyrrolo[2,3-d]pyrimidine-5-carbonitrile 14
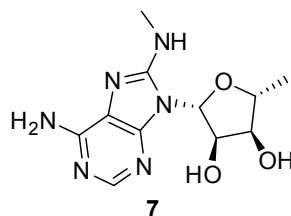
1H-NMR

13C-NMR
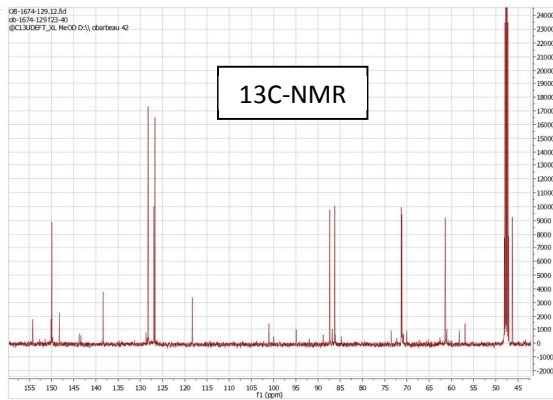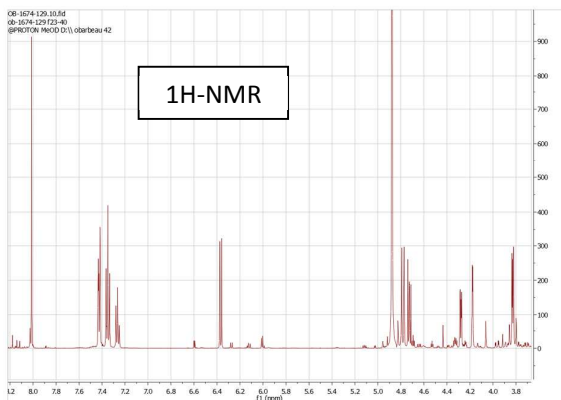
(2R,3R,4S,5R)-2-(6-amino-8-(benzylamino)-9H-purin-9-yl)-5-(hydroxymethyl)tetrahydrofuran-3,4-diol **15**

1H-NMR

17
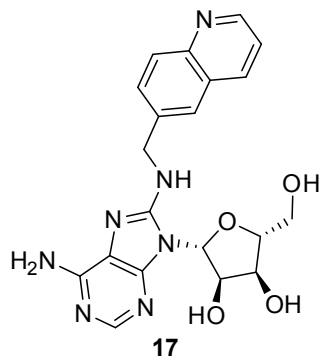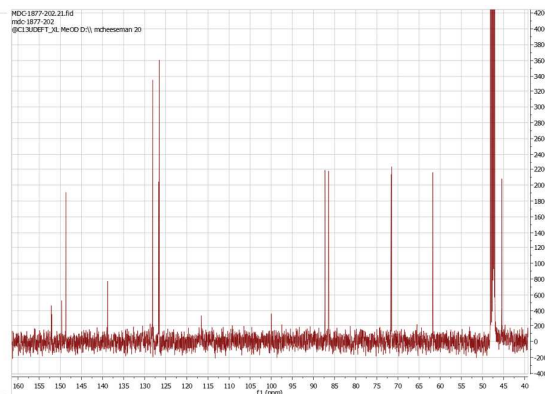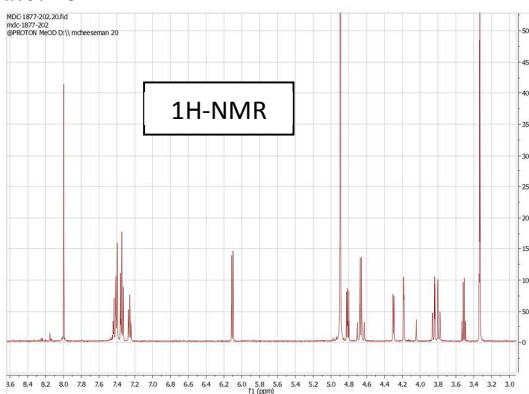
(2R,3R,4S,5R)-2-(6-amino-8-((quinolin-6-ylmethyl)amino)-9H-purin-9-yl)-5-(hydroxymethyl)tetrahydrofuran-3,4-diol **17**

18
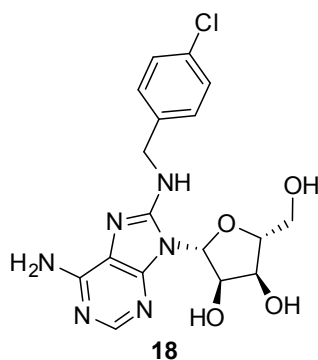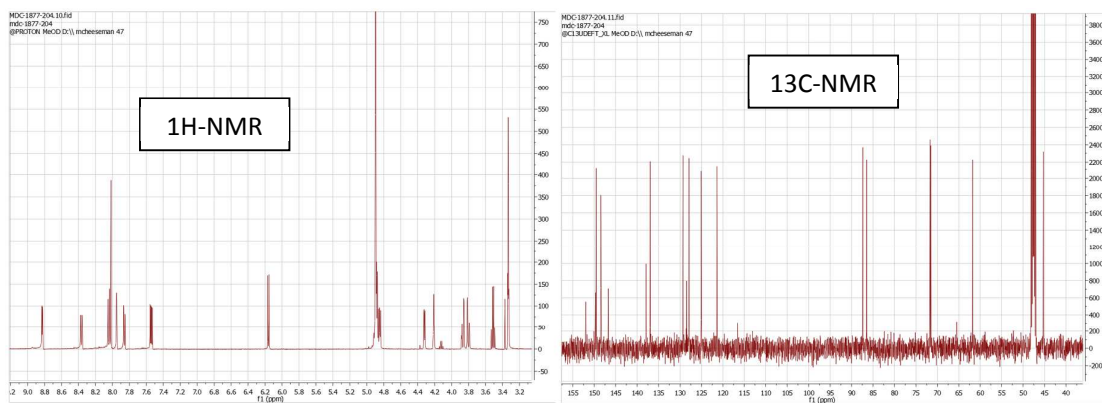
(2R,3R,4S,5R)-2-(6-amino-8-((4-chlorobenzyl)amino)-9H-purin-9-yl)-5-(hydroxymethyl)tetrahydrofuran-3,4-diol **18**

19
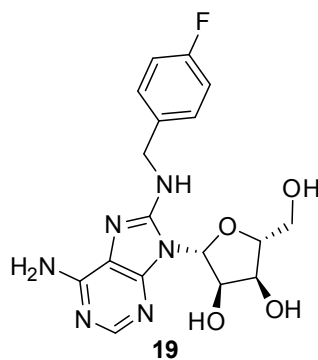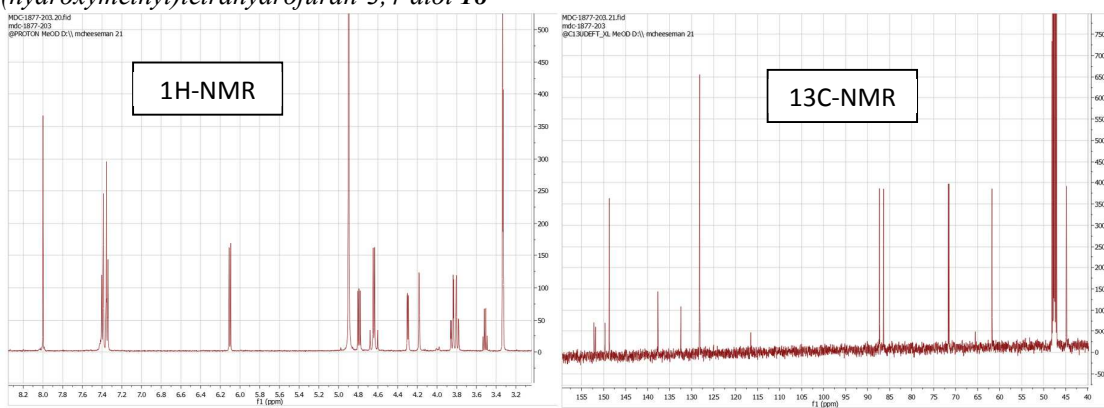
(2R,3R,4S,5R)-2-(6-amino-8-((4-fluorobenzyl)amino)-9H-purin-9-yl)-5-(hydroxymethyl)tetrahydrofuran-3,4-diol **19**

1H-NMR

13C-NMR
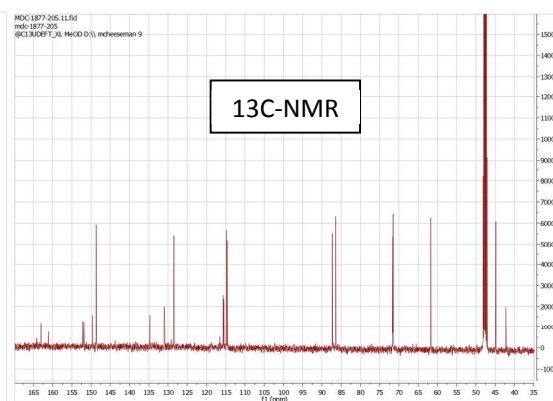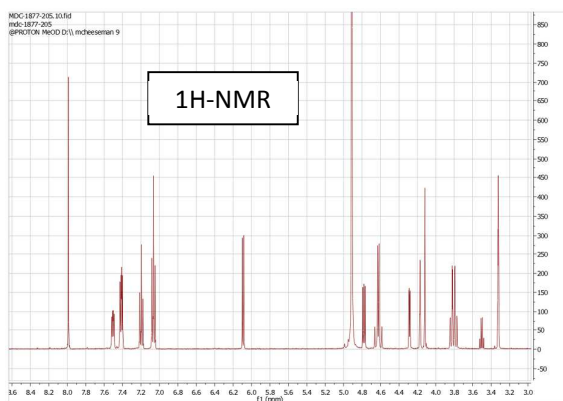
*(2R,3R,4S,5R)-2-(6-amino-8-((4-methylbenzyl)amino)-9H-purin-9-yl)-5-
(hydroxymethyl)tetrahydrofuran-3,4-diol* **20**

1H-NMR

13C-NMR

21
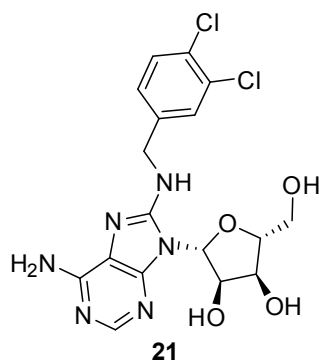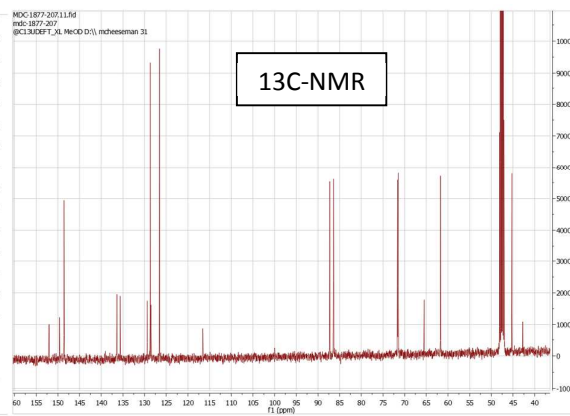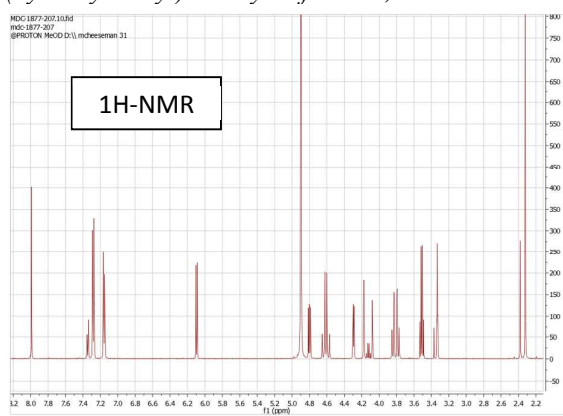
*(2R,3R,4S,5R)-2-(6-amino-8-((3,4-dichlorobenzyl)amino)-9H-purin-9-yl)-5-
(hydroxymethyl)tetrahydrofuran-3,4-diol* **21**

1H-NMR

13C-NMR
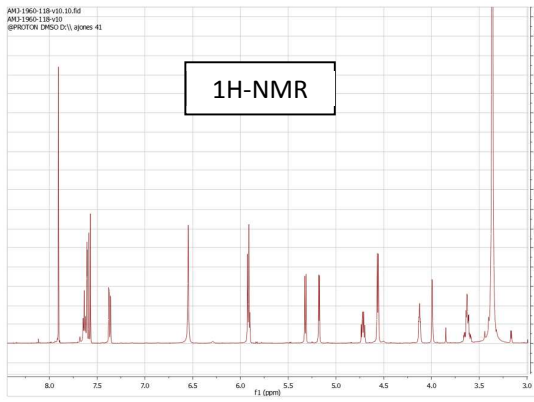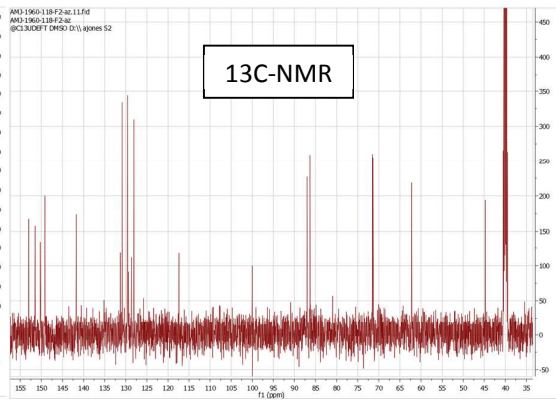
Representative SPR Sensorgrams and Binding Curves
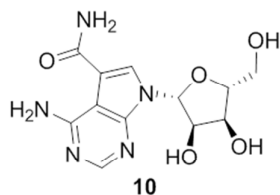
Protein=5206 RU
K_D=3.9 μM
ExpR$_{max}$=35 RU
ThrR$_{max}$=37 RU
Ratio=0.94
Chi^2=0.10
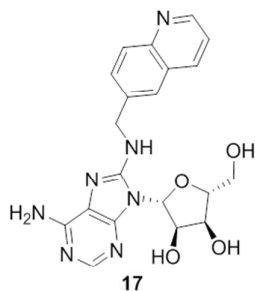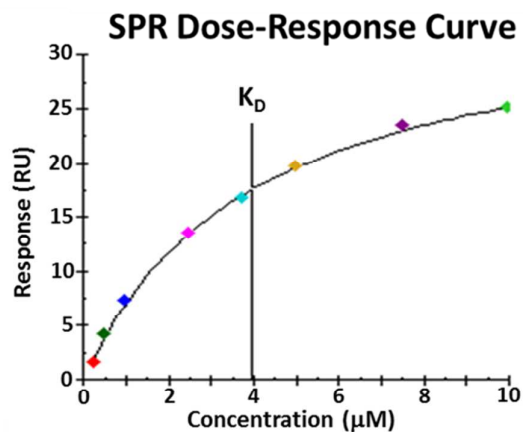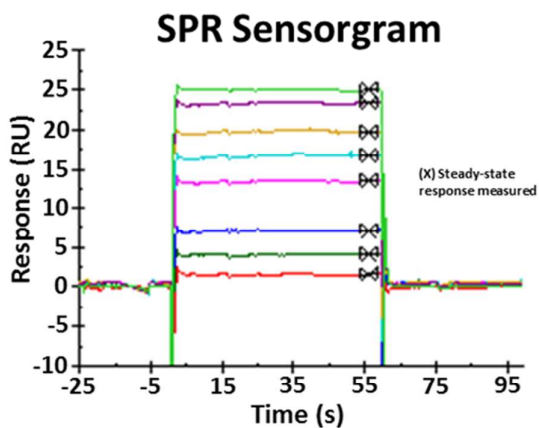
Protein=5118 RU
K_D=0.81 μM
ExpR$_{max}$=61 RU
ThrR$_{max}$=50 RU
Ratio=1.2
Chi^2=0.04
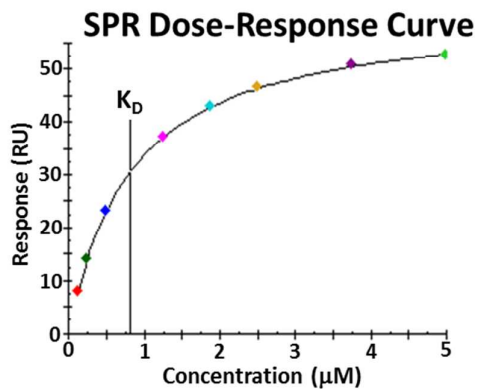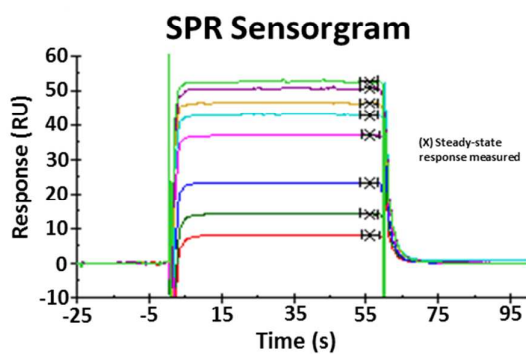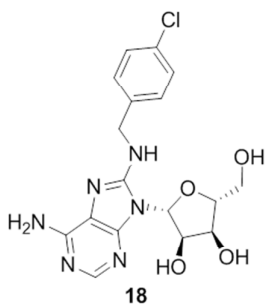
Protein=5118 RU
K_D=0.28 µM
$ExpR_{max}$=53 RU
$ThrR_{max}$=48 RU
Ratio=1.1
Chi^2=0.09

18
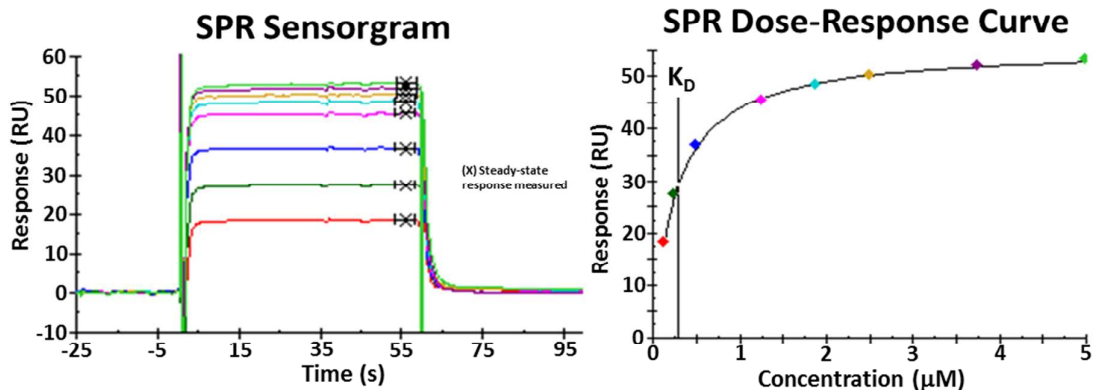
The off-rates for quinoline **17** and *para*-chloro **18** were calculated from the dissociation phase (60-70 s) by fitting the raw data to the first-order rate equation using Excel:

$$R = R_0 \times e^{-k_d(t-t_0)} + R_\infty$$

Quinoline **17**:

$$k_d = 0.45\ s^{-1}\ (0.48 - 0.41\ s^{-1})\ r^2 = 0.98$$
$$t_{1/2} = 1.5\ s\ (1.4 - 1.7\ s)$$

Para-chloro **18**:

$$k_d = 0.36\ s^{-1}\ (0.41 - 0.31\ s^{-1})\ r^2 = 0.88$$
$$t_{1/2} = 1.9\ s\ (1.7 - 2.2\ s)$$

The 95% confidence intervals of the geometric means are quoted in parenthesis.

Fo-Fc electron density figures for ligand-bound HSP72 structures
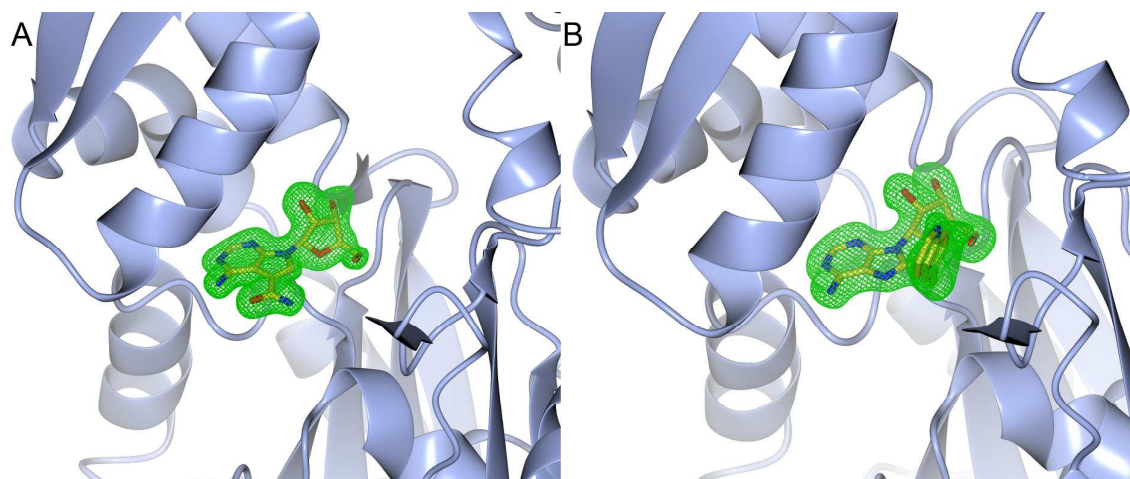
*Fo-Fc electron density maps (green) for HSP72-NBD ligand-bound structures contoured at 3s. A) Sangivamycin, compound **10**. B) Compound **17** HSP72 (blue) is shown in a ribbon representation.*

Data collection and refinement statistics for HSP72 co-crystal structures with ligands.

Ligand	Compound 10	Compound 17
PDB ID	5AQZ	5AR0

Crystals		
Space group	$P2_12_12_1$	$P2_12_12_1$
Lattice constants		
a (Å)	47.94	68.94
b (Å)	89.50	70.21
c (Å)	96.92	84.77
α (°)	90	90
β (°)	90	90
γ (°)	90	90
Data collection		
Beamline	Diamond I04-1	Diamond I24
Date of data collection	29-09-2012	08-12-2012
Wavelength (Å)	0.9200	0.9686
Resolution range (Å)	48.46-1.65	46.49-1.90
(highest-resolution shell values)	(1.68-1.65)	(1.94-1.90)
Observations	283187 (10299)	151157 (3296)
Unique reflections	50487 (2381)	25878 (919)
Completeness (%) - Inner shell	99.7	99.7
Average	99.1	89.3
Outer shell	97.1	51.1
Multiplicity	5.6 (4.3)	5.8 (3.6)
R_{merge} (%)	9.9 (198)	13.6 (113)
I/σ(I)	5.3 (0.3)	4.4 (0.6)
Mean I/σ(I)	7.1 (0.5)	7.7 (1.7)
$CC_{1/2}$[a]	0.997 (0.334)	0.993 (0.400)
Average Mosaicity (º)	0.55	0.15
Structure Solution and Refinement		
No. of copies in ASU	1	1
No. of amino acids	390	379
No. of water molecules	432	203
No. of chloride ions	0	1
No. of ethylene glycol molecules	4	0
No. of glycerol molecules	0	3
No. of DMSO molecules	0	2
R-factor (%)	18.6	17.3
R_{free} (%)	22.1	21.0
Ramachandran plot		
Favored (%)	99.0	99.2
Outliers (%)	0.0	0.0
RMSD bonds (Å)	0.010	0.010
RMSD angles (°)	1.01	1.00

[a] Half-dataset correlation coefficient, see: Karplus, P. A.; Diederichs, K. Linking Crystallographic Model and Data Quality. *Science* **2012,** *336,* 1030-1033.

References for X-ray Materials and Methods:

Kabsch, W. Xds. Acta Crystallogr. Sect. D: Biol. Crystallogr. **2010,** 66, 125-132.

Evans, P. Scaling and assessment of data quality. *Acta Crystallogr. Sect. D: Biol. Crystallogr.* **2006,** 62, 72-82.

Winn, M. D.; Ballard, C. C.; Cowtan, K. D.; Dodson, E. J.; Emsley, P.; Evans, P. R.; Keegan, R. M.; Krissinel, E. B.; Leslie, A. G.; McCoy, A.; McNicholas, S. J.; Murshudov, G. N.; Pannu, N. S.; Potterton, E. A.; Powell, H. R.; Read, R. J.; Vagin, A.; Wilson, K. S. Overview of the CCP4 suite and current developments. *Acta Crystallogr. Sect. D: Biol. Crystallogr.* **2011,** 67, 235-242.

McCoy, A. J.; Grosse-Kunstleve, R. W.; Adams, P. D.; Winn, M. D.; Storoni, L. C.; Read, R. J. Phaser crystallographic software. *J. Appl. Cryst.* **2007,** 40, 658-674.

Emsley, P.; Cowtan, K. Coot: model-building tools for molecular graphics. *Acta Crystallogr. Sect. D: Biol. Crystallogr.* **2004,** 60, 2126-2132.

Bricogne, G.; Blanc, E.; Brandl, M.; Flensburg, C.; Keller, P.; Paciorek, W.; Roversi, P.; Sharff, A.; Smart, O. S.; Vonrhein, C.; Womack, T. O. *BUSTER version 2.11.4. Cambridge, United Kingdom: Global Phasing Ltd.*, **2012**.

Adams P. D., Afonine P. V., Bunkóczi G., Chen V. B., Davis I. W., Echols N., Headd J. J.,Hung L.-W., Kapral G. J., Grosse-Kunstleve R. W., McCoy A. J., Moriarty N. W., Oeffner R., Read R. J., Richardson D. C., Richardson J. S., Terwilliger T. C., Zwart P. H. PHENIX: a comprehensive Python-based system for macromolecular structure solution. *Acta Crystallogr. 2010*, D66, 213–221

Smart, O. S.; Womack, T. O.; Sharff, A.; Flensburg, C.; Keller, P.; Paciorek, W.; Vonrhein, C.; Bricogne, G. *Grade, version 1.2.1. Cambridge, United Kingdom: Global Phasing Ltd.,* http://www.globalphasing.com, 2012.

Bruno, I. J.; Cole, J. C.; Lommerse, R. S.; Rowland, R.; Taylor, R.; Verdonk, M. L. Isostar: A library of information about non-bonded interactions. *J. Comp.-Aided. Mol. Des.* **1997,** 11, 525-537.

Davis, I. W.; Leaver-Fay, A.; Chen, V. B.; Block, J. N.; Kapral, G. J.; Wang, X.; Murray, L. W.; Arendall, W. B., 3rd; Snoeyink, J.; Richardson, J. S.; Richardson, D. C. MolProbity: all-atom contacts and structure validation for proteins and nucleic acids. *Nucleic Acids Res.* **2007,** 35, W375-W383.

Potterton, E.; McNicholas, S.; Krissinel, E.; Cowtan, K.; Noble, M. The CCP4 molecular-graphics project. *Acta Crystallogr D Biol Crystallogr* **2002,** 58, 1955-7.
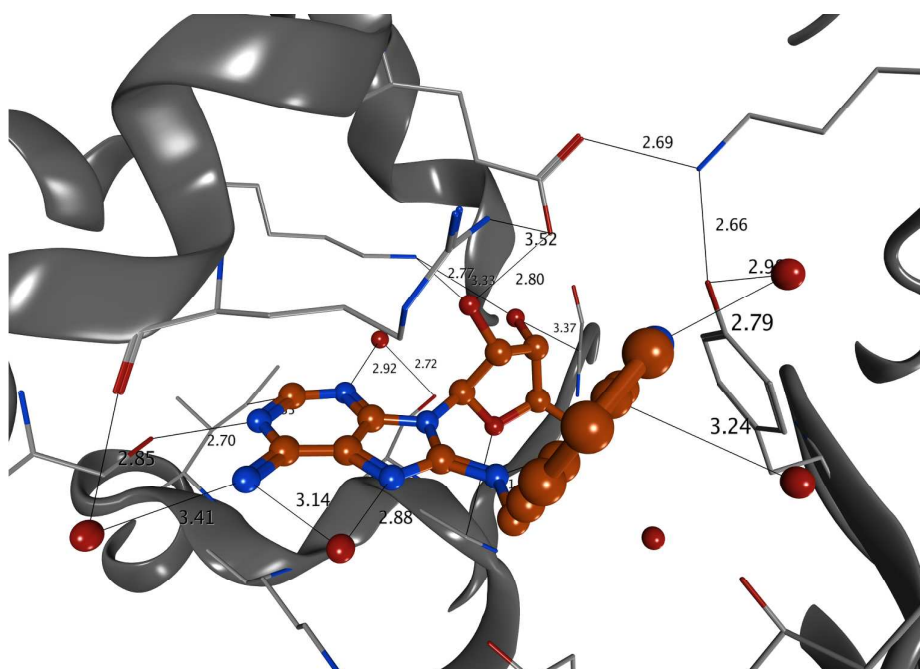
Complete Binding Contacts of Nucleoside ligands for HSP70

**Figure S1** All Close Contacts in the Sangivamycin **10**/HSP72-NBD Co-Crystal Structure
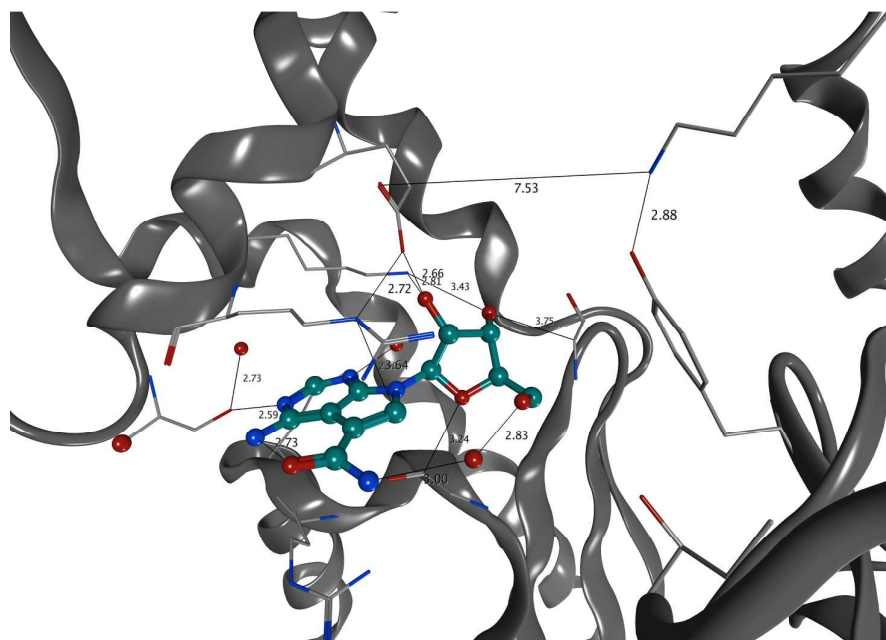
All distances are in Angstoms. The red spheres represent water molecules

**Figure S2** All Close Contacts in the Quinoline **17**/HSP72-NBD Co-Crystal Structure

All distances are in Angstoms. The red spheres represent water molecules

Figure S3 Overlay of ADP/Pi HSP-72 NBD co-crystal structure (copper) and Sangivamycin **10** HSP72 NBD co-crystal (white) highlighting all key binding residues
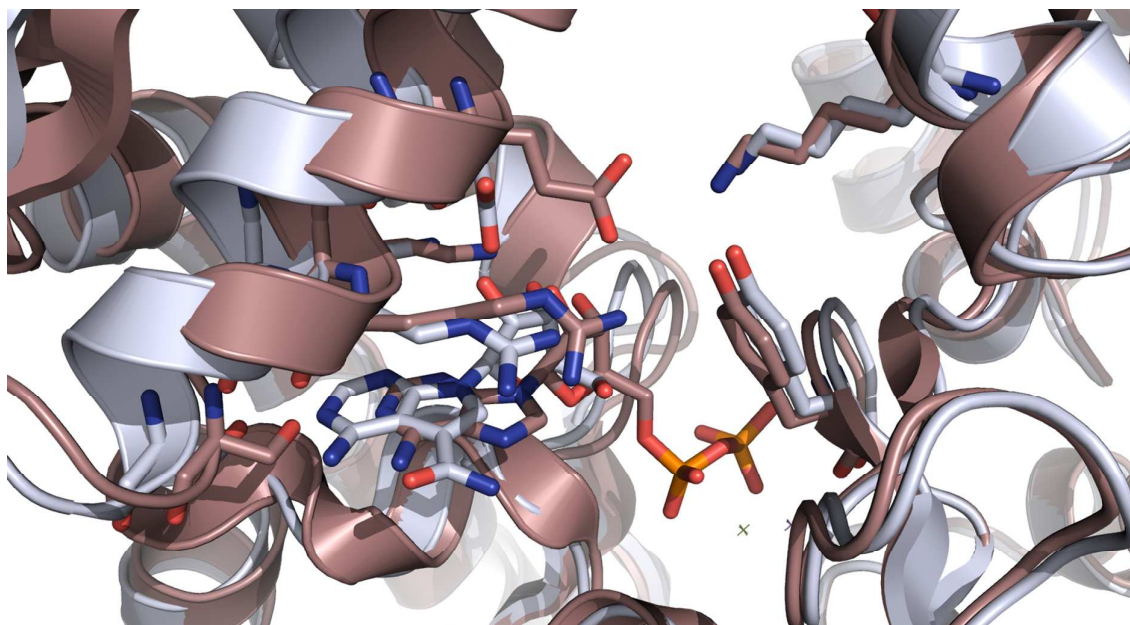
Figure S4 Overlay of ADP/Pi HSP-72 NBD co-crystal structure (copper) and 8-Quinoline **17** HSP72 NBD co-crystal (grey) highlighting all key binding residues
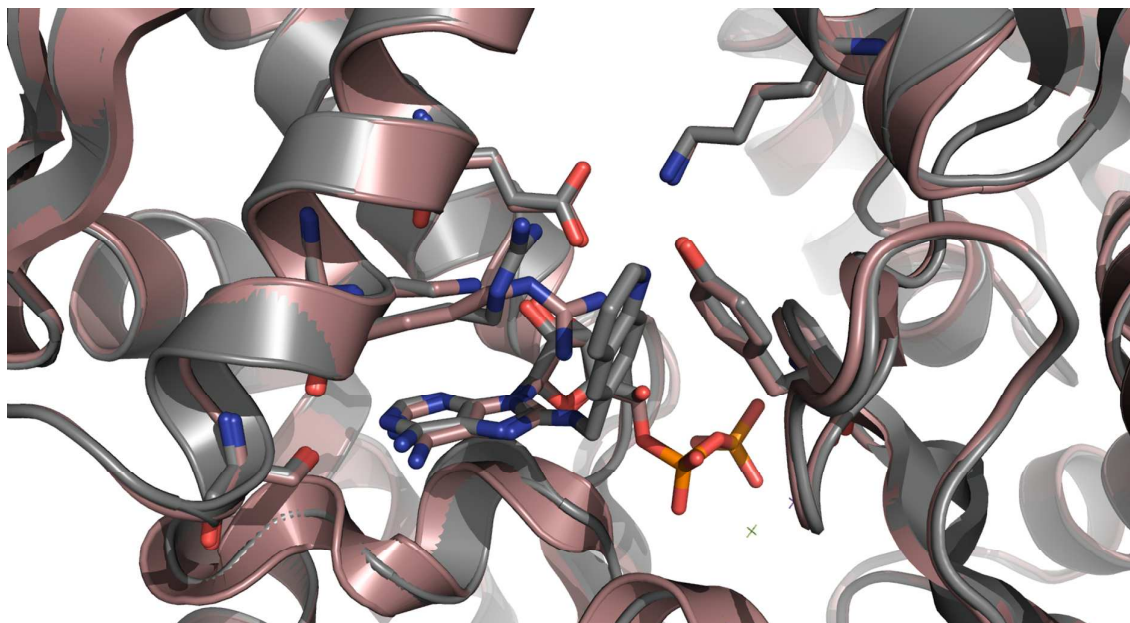
Figure S5 Overlay of Sangivamycin **10** HSP-72 NBD co-crystal structure (white) and 8-Quinoline **17** HSP72 NBD co-crystal (grey) highlighting all key binding residues